Journal of Catalysis **210,** 116–126 (2002)
doi:10.1006/jcat.2002.3658

Push–Pull Mechanism of Hydrodenitrogenation over Silica-Supported MoP, WP, and MoS_2 Hydroprocessing Catalysts

P. Clark,* X. Wang,* P. Deck,† and S. T. Oyama*,†,[1]

*Environmental Catalysis and Materials Laboratory, Department of Chemical Engineering, Virginia Polytechnic Institute and State University, Blacksburg, Virginia 24061-0211; and †Department of Chemistry, Virginia Polytechnic Institute and State University, Blacksburg, Virginia 24061-0211

Received January 9, 2002; revised April 26, 2002; accepted May 2, 2002

The mechanism of liquid-phase catalytic hydrodenitrogenation at 3.1 MPa on silica-supported molybdenum phosphide, MoP/SiO_2, and tungsten phosphide, WP/SiO_2, was studied using a series of pentylamines of different structures. The reactivity pattern suggested that removal of nitrogen occurred primarily by an E2 elimination mechanism involving acidic and base sites on the catalyst surfaces in a push–pull process. Infrared spectroscopy and temperature-programmed reaction studies of ethylamine indicated that alkyl ammonium species formed on Brønsted acid sites were intermediates in the reaction. Similar results were obtained with a reference MoS_2/SiO_2 sample tested at the same conditions. This suggested that sulfur was probably present on the active surface and assisted in the removal of sulfur.

Key Words: **hydrodenitrogenation; mechanism; tungsten phosphide; molybdenum sulfide; pentylamine.**

INTRODUCTION

Transition-metal phosphides have recently been reported to be effective hydroprocessing catalysts, extending the range of materials known to be active for this class of reactions. In particular MoP (1–4), WP (5, 6), Co_2P (7), and Ni_2P (8) have been shown to give high conversions in hydrodesulfurization (HDS), and especially hydrodenitrogenation (HDN), of model petroleum feedstocks. Little is known about the nature of these catalytic materials, and studies to elucidate their behavior are of practical and fundamental interest. We have undertaken the present investigation to understand the mechanism by which the phosphide catalysts carry out the HDN reaction of alkylamines.

The subject of HDN on sulfides, carbides, and nitrides has recently been comprehensively reviewed by Prins (9). Elucidation of the mechanism of HDN is complicated for several reasons. Not only is the reaction affected by the conditions at which it is run, such as hydrogen pressure, residence time, and the presence of H_2S, but also the catalyst may be complex and may possess multiple functionalities, such as hydrogenation and hydrogenolysis sites (10). It is likely that the mechanism and rate of reaction will depend ultimately on the nature of its interaction with the reacting molecule. The most well known mechanism of denitrogenation is the Hoffmann degradation of amines (11), but there are a number of other possibilities (12–14) such as nucleophilic substitution (S_N1, S_N2), elimination (E1, E2), and metallacycle or metal alkyl formation pathways (Scheme 1). The mononuclear pathways (S_N1 and E1) start with the generation of a carbocation by quaternization of an amine followed by cleavage of ammonia. Nucleophilic substitution occurs by attack of a nucleophile (HS^-) on the carbenium ion (the original α-carbon), whereas elimination occurs by abstraction of a proton by the nucleophile (from the original β-carbon). The binuclear pathways (S_N2 and E2) begin with the formation of the quaternized ammonium compound as in the mononuclear case, but without scission of ammonia. Nucleophilic substitution occurs by attack of a nucleophile on the α-carbon whereas elimination (E2) occurs by attack of a base on a proton attached to a β-carbon to form an olefin. The pathways involving reactions with metals (C–N oxidative addition and metal alkyl formation) require activation of the α-carbon to the nitrogen (15–17). These pathways likely occur with metallic catalysts such as Rh, Pd, or Ru but are not preferred with the phosphide or sulfide catalysts considered here. To ascertain the operative mechanism (S_N1, E1, S_N2, or E2) on the catalysts, use was made of the method of Breysse (12–14) which employed a series of pentylamines of different structure. The original work was carried out in the vapor phase, and we have adapted the method to employ more realistic conditions of liquid phase and high pressure (3.1 MPa). Comparison is made to a simple sulfide deposited on a noninteracting support, MoS_2/SiO_2, to avoid complications due to promoters and acidic supports.

[1] To whom correspondence should be addressed. E-mail: oyama@vt.edu.

0021-9517/02 $35.00

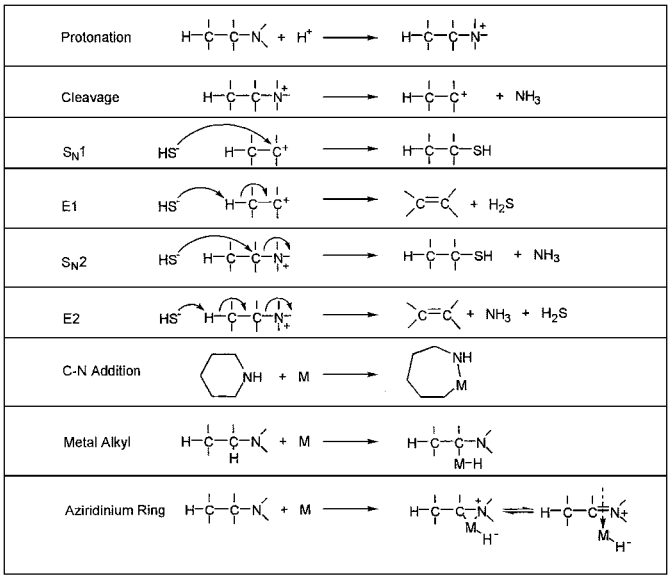

SCHEME 1. Mechanisms and intermediates in C–N bond cleavage.

EXPERIMENTAL

Supported phosphides were prepared by incipient wetness impregnation of silica with aqueous metal phosphate precursors, followed by controlled reduction in flowing hydrogen. The preparation, characterization, and catalytic activity of the silica-supported phosphides were reported in an earlier paper (18). Briefly, stoichiometric quantities of ammonium paramolybdate, $(NH_4)_6Mo_7O_{24} \cdot 4H_2O$ (Aldrich, 99%), or ammonium metatungstate, $(NH_4)_6W_{12}O_{39} \cdot xH_2O$ (Aldrich, 90%), were combined with ammonium phosphate, $(NH_4)_2HPO_4$ (Aldrich, 99%), in distilled water, and the solution was used to impregnate the silica support. Quantities of reagents were used to give weight loadings of 13% MoP/SiO_2 and 20% WP/SiO_2, corresponding to molar loadings of 1.16 mmol metal/g SiO_2. The moist paste obtained after impregnation was calcined in air at 773 K for 6 h. The resulting precursor phosphates were reduced to phosphides in quartz U-tube reactors (1 cm o.d.) using linear temperature ramps in flowing hydrogen. Hydrogen flow was set at 650 μmol s^{-1} g^{-1} starting material (e.g., 300 cm^3(NTP) min^{-1} H_2 flow for a 0.300 g sample) for all syntheses. The MoP/SiO_2 required a final reduction temperature of 850 K and the WP/SiO_2 required a final temperature of 1000 K. After reduction, the phosphides were cooled to room temperature under 65 μmol s^{-1} helium and typically were passivated progressively by flowing 78 μmol s^{-1} of 0.1% O_2/He overnight, followed by 13 μ mol s^{-1} of 0.5% O_2/He for 2 h, and then allowing ambient air to diffuse into the reactor tube for 24 h before collecting the samples.

Samples of 5.6 wt% MoS_2/SiO_2 corresponding to 0.368 mmol metal/g SiO_2 were prepared by sulfiding MoO_3/SiO_2 for 2 h in a stream of 10% H_2S/H_2 at 678 K. The sulfide samples used for hydroprocessing and O_2 chemisorption were sulfided directly from the oxide within the catalytic reactor using the same procedure.

All gases were supplied by Air Products. Hydrogen, helium, and carbon monoxide were all 99.999% pure and were passed through a water trap (Alltech) before contacting the sample. Specialty mixtures, including 0.5% O_2/He, 30% N_2/He, and 10% H_2S/H_2, were used as received.

The total dynamic CO uptake was measured by passing pulses of CO (5.6 μmol) in a stream of 40 μmol s^{-1} helium over samples at room temperature (RT). Measurements were performed *ex situ* on air-exposed samples reduced to 723 K for 2 h. Oxygen uptakes were measured in the same manner except that the chemisorption temperature was that of dry ice/acetone (195 K) and the O_2 uptake was multiplied by a factor of 2 to account for dissociative adsorption on the surface. Surface area measurements by N_2 adsorption were performed with a Micromeritics 2000 sorption unit.

X-ray diffraction (XRD) spectra were collected with a Scintag XDS-2000 X-ray diffractometer using Ni-filtered Cu $K\alpha$ ($\lambda = 0.1541$ nm) radiation. Scans were collected at a rate of 0.035° 2θ s^{-1} and in increments of 0.03° 2θ.

The mechanism of HDN was studied by hydrodenitrogenation of solutions containing 2000 wppm N (wppm = parts per million by weight) as *n*-pentylamine ($C_5H_{13}N$, Acros, 99%), *tert*-pentylamine (Acros, 98%), or *neo*-pentylamine (TCI) dissolved in tetradecane (Fisher, 99%). These reactions were carried out at 3.1 MPa as a function of temperature for each catalyst. The pentylamine feed solutions also contained 3000 wppm S as dimethyldisulfide ($C_2H_6S_2$, Aldrich, 99%), as well as 2000 wppm *n*-octane (C_8H_{18}, Aldrich, 99%) as an internal standard.

The basis used for the calculation of catalytic reaction results was the percent of reactant converted to a given product, where all of the detected reactant and product species are counted as 100%. HDN was defined as the conversion of the amine to hydrocarbon products and so did not include condensation (transalkylation) products. The carbon balances on the amine reactants and their products were typically 90% ± 10%. The balance was low because only the liquid-phase products were analyzed. Gas–liquid equilibria were considered in the liquid samples after collection to help account for the volatility of the C_5 hydrocarbons and amines at ambient conditions (19). Small amounts of light products were found in dry-ice temperature condensate from the hydrogen (vapor) effluent, but it was not possible to accurately quantify this material because complications arose from carryover of the liquid-phase solvent tetradecane in the gas stream.

The composition of hydroprocessing liquids was identified with a Hewlett–Packard 5890A gas chromatograph (equipped with a CP Sil 5B column) on samples collected at 2–3-h intervals. Steady state was typically achieved after about 60 h of reaction time at a given condition. Reaction

products were identified through matching of retention times with commercially available standards, as well as by GC/MS analysis. The GC/MS combined a Fisons Carlo Erba 8060 series gas chromatograph, using a HP-5MS 5% phenylmethylsiloxane stationary phase, with a VG Quattro triple quadrupole mass spectrometer operated in the electron impact–positive ion mode.

To start a catalytic reaction, phosphide catalysts were pretreated in 100 μmol s^{-1} hydrogen at 723 K and 1 atm pressure for 2 h, while the sulfide catalyst was presulfided with a 10% H_2S/H_2 mixture at 678 K and 1 atm pressure for 2 h. After the pretreatment, the conditions were set to 3.1 MPa (450 psig), a hydrogen flow rate of 100 μmol s^{-1} (150 cm^3 NTP min^{-1}), a liquid feed rate of 0.0833 cm^3 s^{-1} (5 cm^3 min^{-1}), and the desired temperature. For amine reactions, the amounts of catalysts used were 3.3 g of MoS_2/SiO_2, 1.4 g of MoP/SiO_2, and 3.1 g of WP/SiO_2. These amounts corresponded to roughly similar quantities (56, 70, and 58 μmol, respectively) of chemisorption sites. Once started, the individual catalysts were used for extended sets of conditions (i.e., different feeds and temperatures). The duration of the experiments was lengthy, requiring several weeks, but standard conditions were repeated periodically to verify that no deactivation occurred. Results from repeated conditions were similar and were averaged to obtain the reported values.

Diffuse reflectance Fourier transform infrared (FTIR) spectra of ethylamine in the gas phase and adsorbed on the WP/SiO_2 catalyst and the SiO_2 support were measured with a Bio-Rad FTS 60A spectrometer equipped with a Spectra-Tech HTEC-0030-103 high-temperature environmental chamber. The finely powdered catalysts were pressed flat in the sample holder of the environmental chamber and pretreated as for reaction. They were then exposed to 3000 wppm S in the form of H_2S in H_2 at 553 K followed by six ethylamine pulses (20 μmol) in H_2. Spectral acquisition consisted of 1024 scans at different temperatures after purging with H_2. The catalyst sample data were normalized by the background spectrum acquired using a blank KBr sample.

Temperature-programmed desorption (TPD) of ethylamine from the WP/SiO_2 catalyst was carried out using H_2 as the carrier gas. As with the FTIR measurements, the sample was pretreated as for reaction and then exposed to an H_2S/H_2 stream with a concentration of 3000 wppm S. The sample was purged in H_2 and the adsorption of ethylamine was carried out in pulse mode as before. The saturated sample was again purged in H_2 and the temperature-programmed experiment was carried out using a linear temperature increase of 0.135 K s^{-1} to a final temperature of 1273 K. The desorbing species from the catalyst were monitored with a mass spectrometer during the heating. The areas for the desorbing species were compared with the areas from calibrated pulses of reference gases.

RESULTS

Preparation and Characterization of Catalysts

The catalysts were prepared and characterized as described previously (18). Briefly, the phosphides, MoP/SiO_2 and WP/SiO_2, were obtained by the temperature-programmed reduction of supported phosphate precursors. The catalysts were shown to be single-phase materials by ^{31}P nuclear magnetic resonance spectroscopy. The sulfide, MoS_2/SiO_2, was obtained by sulfidation of a supported oxide precursor. A summary of surface area and chemisorption properties is provided in Table 1.

A study of the reactivity of a series of pentylamines was carried out to explore the effect of amine structure on the HDN reaction. The results for each individual amine are presented in the following.

n-Pentylamine

The product distributions for *n*-pentylamine HDN on silica-supported MoP, WP, and MoS_2 are presented in Fig. 1. The species favored at the lowest temperature in each case was the condensation product dipentylamine. As temperature increased, pentane appeared along with small amounts of pentenes, pentanethiol, and tripentylamine. Total *n*-pentylamine conversions at all temperatures except 513 K increased in the order $MoP/SiO_2 < MoS_2/SiO_2 < WP/SiO_2$; however, the production of hydrocarbons increased in the order $MoP/SiO_2 < WP/SiO_2 < MoS_2/SiO_2$. The MoP/SiO_2 catalyst (Fig. 1a) was the least active by both measures. Comparatively, the WP/SiO_2 catalyst (Fig. 1b) had a higher propensity for condensation than MoS_2/SiO_2, while the MoS_2/SiO_2 catalyst (Fig. 1c) had higher hydrocarbon production.

TABLE 1

Surface Area and Chemisorption Characteristics of Fresh and Spent Silica-Supported Catalyst Samples

Sample	Surface area,[a] fresh	CO uptake[b]	
		Fresh	Spent[c]
SiO_2 blank	91	0	0
MoS_2/SiO_2	93[d]	18[e]	—
MoP/SiO_2	50	50	26
WP/SiO_2	62	19	10.8

[a] Surface area in m^2 g^{-1} catalyst; passivated catalysts; degassed in vacuum at 273 K for 24 h.

[b] Uptake at room temperature in μmol g^{-1}; samples pretreated at 723 K in H_2.

[c] Uptake at room temperature following hydrodenitrogenation of pentylamines.

[d] As oxide: MoO_3/SiO_2.

[e] O_2 uptake at 78 K; sample presulfided at 678 K in 10% H_2S/H_2.

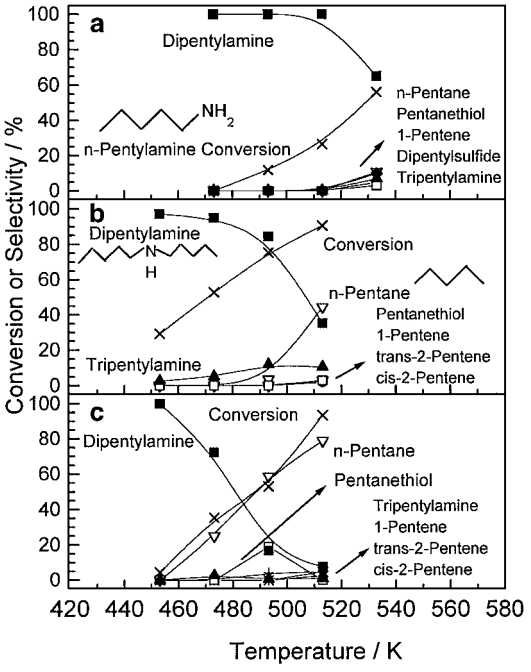

FIG. 1. Product distribution in the hydrogenolysis of *n*-pentylamine on (a) MoP/SiO_2, (b) WP/SiO_2, and (c) MoS_2/SiO_2 catalysts: (×) conversion, (■) dipentylamine, (▽) *n*-pentane, (▲) tripentylamine, (○) pentenes, and (□) pentanethiol.

The amounts and distributions of olefins at 533 K are summarized in Table 2, along with equilibrium concentrations estimated by thermodynamic calculations for this temperature. The predominant olefin formed on all catalysts was 1-pentene. *Cis*- and *trans*-2-pentenes were observed for the WP/SiO_2 and MoS_2/SiO_2 catalysts at higher temperatures (513 K). In no cases were isopentene isomers observed.

Overall, the hydrocarbon distribution was consistent with the occurrence of HDN by an elimination reaction followed by dehydrogenation. However, significant amounts of pentanethiol were also found at 493 K on the MoS_2/SiO_2 catalyst, demonstrating the presence of N–S exchange as well.

TABLE 2

Olefin Production and Distribution for *n*-Pentylamine HDN at 513 K

Sample	Total olefins, %[a]	% Selectivity[b]		
		1-Pentene	*trans*-2-Pentene	*cis*-2-Pentene
MoP/SiO_2[c]	3	100	0	0
WP/SiO_2	6	42	30	28
MoS_2/SiO_2	12	39	39	22
Equilibrium	—	7	69	24

[a] Percent of *n*-pentylamine converted to olefins.
[b] Percent of total olefin.
[c] MoP results are from 533 K. Total hydrocarbons for MoP at 513 K = 0.

tert-Pentylamine

The product distributions for *tert*-pentylamine HDN on silica-supported MoP, WP, and MoS_2 are presented in Fig. 2. Hydrocarbons were the only products of *tert*-pentylamine HDN, with olefins being preferred at lower temperatures, and the alkane 2-methylbutane becoming more important at higher temperatures. The order of activity of the catalysts increased as $MoP/SiO_2 < WP/SiO_2 < MoS_2/SiO_2$, with the MoP catalyst (Fig. 2a) being significantly less active than either the WP (Fig. 2b) or MoS_2 (Fig. 2c) catalysts. The relative amount of 2-methyl-2-butene was always greater than 2-methyl-1-butene on each catalyst. Di(*tert*-pentyl)amine was not observed, in agreement with previous results (12), and its absence is attributed to steric effects.

neo-Pentylamine

The product distributions for *neo*-pentylamine HDN on silica-supported MoP, WP, and MoS_2 are presented in Fig. 3. The initial product formed at low temperatures/conversions was di(*neo*-pentyl)amine. This molecule was the only product detected on the MoP catalyst (Fig. 3a). On WP (Fig. 3b) and MoS_2 (Fig. 3c), 2,2-dimethylpropane was observed at higher temperatures and was the only hydrocarbon product detected. The order of reactivity of the catalysts in terms of both total conversion and the formation of hydrocarbons increased in the order $MoP/SiO_2 < WP/SiO_2 < MoS_2/SiO_2$. Small amounts of 2,2-dimethylpropanenitrile were detected in products

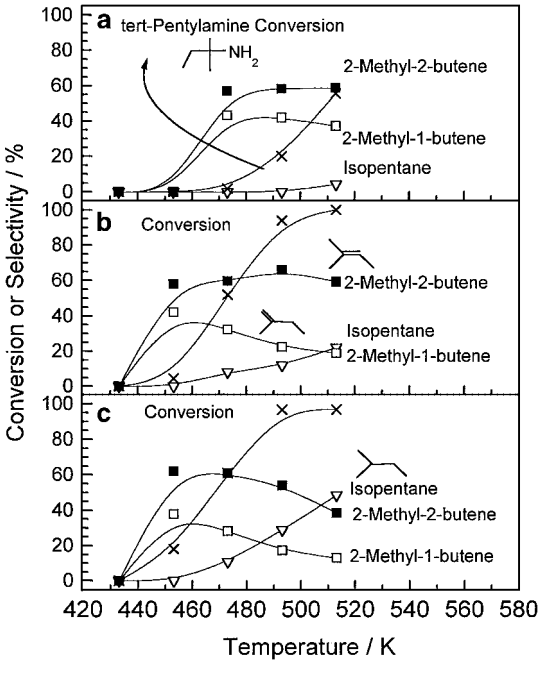

FIG. 2. Product distribution in the hydrogenolysis of *tert*-pentylamine on (a) MoP/SiO_2, (b) WP/SiO_2, and (c) MoS_2/SiO_2 catalysts: (×) conversion, (■) 2-methyl-2-butene, (□) 2-methyl-1-butene, and (▽) *n*-pentane.

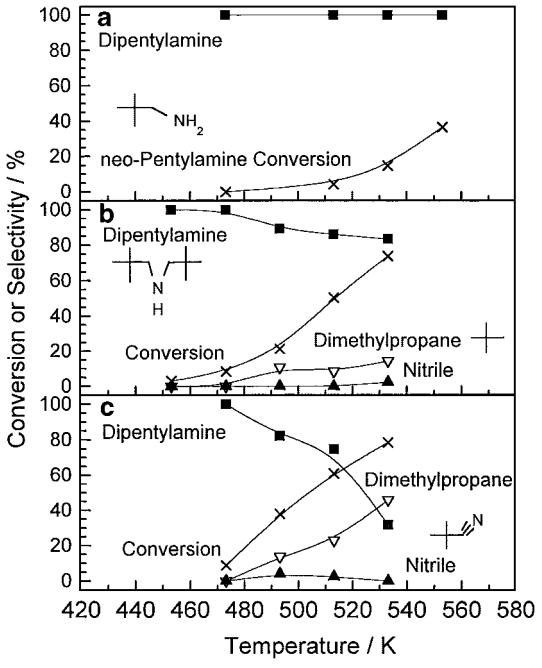

FIG. 3. Product distribution in the hydrogenolysis of *neo*-pentylamine on (a) MoP/SiO_2, (b) WP/SiO_2, and (c) MoS_2/SiO_2 catalysts: (×) conversion, (■) di(*neo*-pentyl)amine, (▽) dimethylpropane, and (▲) 2,2-dimethylpropylnitrile.

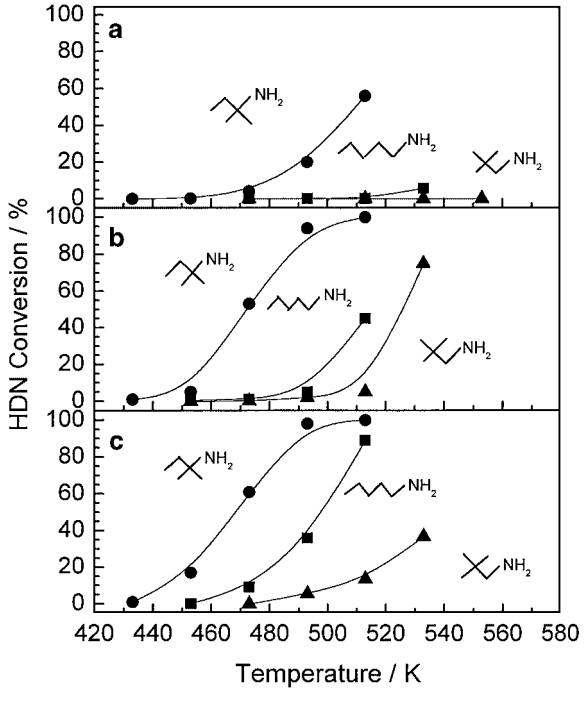

FIG. 4. Total HDN conversion of pentylamines over (a) MoP/SiO_2, (b) WP/SiO_2, and (c) MoS_2/SiO_2 catalysts.

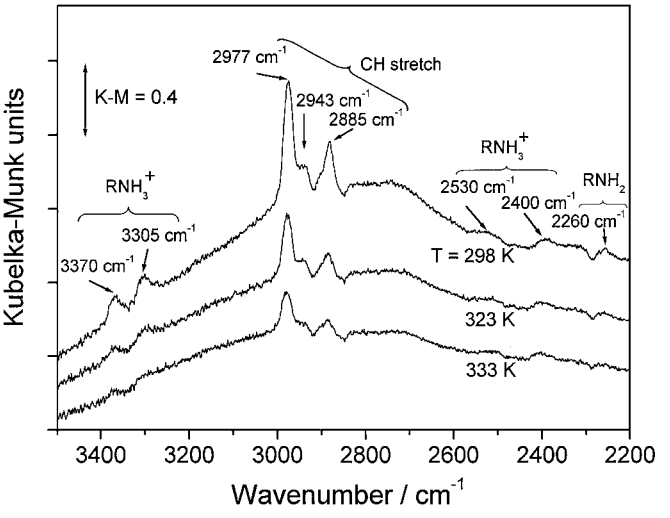

FIG. 5. Fourier transform infrared spectra of ethylamine adsorbed on WP/SiO_2.

produced by WP and MoS_2 containing catalysts. Thus, *neo*-pentylamine is the only molecule for which a nitrile product was observed in this study.

An overall summary of the reactivity of the MoP/SiO_2, WP/SiO_2, and MoS_2/SiO_2 catalysts in HDN is provided in Fig. 4. The data in that figure are extracted from Figs. 1–3 to show only conversion to denitrogenated hydrocarbon products.

The FTIR spectra at different temperatures of adsorbed ethylamine on the WP/SiO_2 catalyst exposed to H_2S are shown in Fig. 5. Major features are seen at 2260, 2400, 2530, 2885, 2943, 2977, 3305, and 3370 cm^{-1}. These features diminish in intensity as the temperature is raised from 298 to 333 K.

FTIR spectra taken at similar conditions on the SiO_2 support are shown in Fig. 6. Here features are observed at 2260,

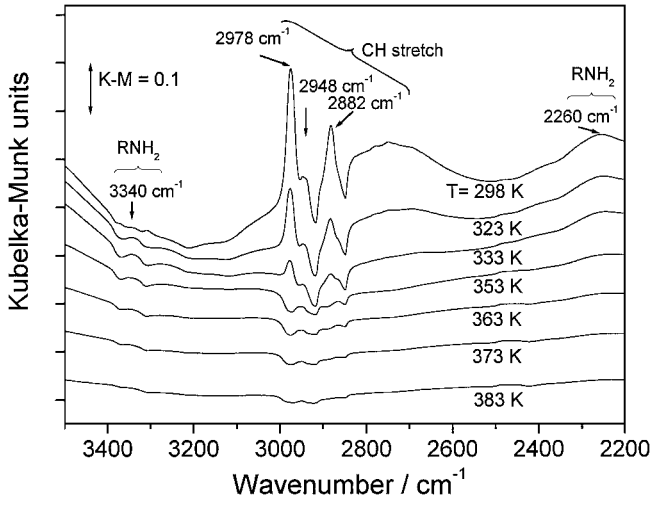

FIG. 6. Fourier transform infrared spectra of ethylamine adsorbed on SiO_2.

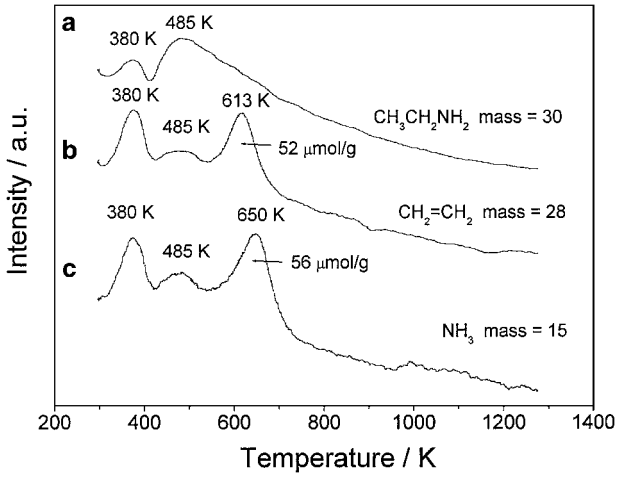

FIG. 7. Temperature-programmed desorption traces of ethylamine from WP/SiO_2: (a) desorption of ethylamine, (b) desorption of ethylene, and (c) desorption of ammonia.

2882, 2948, 2978, and 3340 cm^{-1}, and again these diminish in intensity as the temperature is increased. There was no difference in the spectra with H_2S pretreatment, indicating that no acid sites are formed by the action of H_2S on the SiO_2.

The TPD traces of ethylamine from WP/SiO_2 exposed to H_2S are shown in Fig. 7. The figure displays the mass spectrometer signals from three masses representing ethylamine (mass = 30), ethylene (mass = 28), and ammonia (mass = 15) as a function of temperature. The assignment of these masses was checked by examination of secondary masses. For example, the fragmentation pattern of ethylamine has the following distribution: mass 30 (100), mass 28 (32), mass 44 (18), mass 45 (17), mass 27 (15), and mass 15 (11), where the numbers in parentheses indicate relative intensity. Because of the high intensity for mass 30, this was the primary signal monitored for ethylamine. In order to distinguish it from ethane, which also has mass 30, the signal was compared to that of mass 45. The topmost trace (Fig. 7, curve a), corresponding to the desorption of the parent compound ethylamine, shows a relatively sharp peak at 380 K and a broad feature with a maximum at 485 K. The other traces (Fig. 7, curves b and c) show corresponding signals which are partially due to the fragmentation of the parent compound. However, the traces also show distinct peaks at 613 K for ethylene and 650 K for ammonia, indicating the separate production of these species. Integration of the area under these peaks and quantitation by comparison to the signals obtained from injected standards give desorption amounts of 52 μmol g^{-1} for ethylene and 56 μmol g^{-1} for ammonia.

DISCUSSION

The *ex situ* chemisorption characteristics and BET surface areas of the catalyst samples are summarized in Table 1. The surface area of the MoS_2/SiO_2 catalyst (93 m^2 g^{-1}) precursor was close to that of the support (91 m^2 g^{-1}) because its loading was low. The surface areas of the MoP/SiO_2 (50 m^2 g^{-1}) and WP/SiO_2 (62 m^2 g^{-1}) samples were significantly decreased from that of the support, a common finding for phosphorus-promoted supported catalysts (20, 21). This is presumably an effect of pore blocking by the supported catalyst compounds as surface area decreases with loading (3). Chemisorption quantities of O_2 and CO for the fresh catalysts were moderate and were found to decrease somewhat after catalytic reaction for the phosphides. Chemisorption measurements taken after catalytic reaction were carried out on recovered samples washed in hexane and rereduced at 723 K for 2 h. The fresh MoP/SiO_2 had a larger CO uptake (50 μmol g^{-1}) than the WP/SiO_2 (19 μmol g^{-1}). This probably was the result of the lower synthesis temperature required for MoP/SiO_2 (850 K) than WP/SiO_2 (1000 K), which reflects the relative reducibilities of the Mo and W precursors. The dispersion of MoP/SiO_2 (4.9%) was consequently larger than that of WP/SiO_2 (2.0%). As noted earlier, the reactivity work presented here is based on approximately equal chemisorption sites loaded in the catalytic reactor. The sites are titrated by the adsorption of CO at RT on the phosphides and O_2 at low temperature for the sulfides. These are reasonable techniques. On the phosphides our previous characterization work (18) showed that the CO uptake is close to the expected metal site density obtained from the crystallite sizes. Moreover, the conversion in HDS and HDN was invariant with loading when equal sites were loaded in the reactor (3). On the sulfides careful studies have clearly shown that on unpromoted MoS_2 the low-temperature chemisorption of O_2 tracked linearly with activity (22–26). This is another reason for choosing a simple system like MoS_2/SiO_2 for comparison.

It is generally recognized that HDN is more difficult than HDS in hydroprocessing because of the higher strength (by 12–38 kJ mol^{-1}) of C–N bonds versus C–S bonds (27). The high activity of the phosphide catalysts for HDN was unusual (18) and prompted investigation of the mechanism of HDN. A method described by Breysse's group (12–14) utilizing a series of pentylamines of different structure was adapted to high-pressure, liquid-phase conditions in our study. The amines consisted of *n*-pentylamine, *tert*-pentylamine, and *neo*-pentylamine and their structure and attributes are described in Table 3. For each amine the table lists the number of hydrogen atoms on the α- and β-carbons, the degree of steric hindrance, and the relative stability of carbocations and carbanions formed on removal of the amine group.

The expected relative reactivities of the pentylamines are summarized in Table 4, as described by Cattenot *et al.* (12). *neo*-Pentylamine contains no β-hydrogen atoms and is sterically hindered, so is expected to be the least reactive molecule in the series. *tert*-Pentylamine has the greatest number of β-hydrogen atoms and forms the most stable

TABLE 3

Relative Properties of Pentylamines for HDN Reaction

Reactant	Structure	Number of α-hydrogens	Number of β-hydrogens	Steric hindrance	Carbocation stability	Carbanion stability
n-Pentylamine	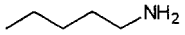	2	2	Low	Low	High
tert-Pentylamine	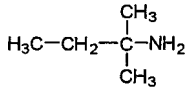	0	8	High	High	Low
neo-Pentylamine	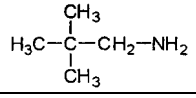	2	0	Med	Med	Med

carbocation counterpart, so it is the most reactive molecule in the series. *n*-Pentylamine has an intermediate number of β-hydrogen atoms, is the least sterically hindered, and is expected to have intermediate activity. Carbocations of *neo*-pentylamine and *n*-pentylamine are expected to have similar stability.

The complete conversion and selectivity results were presented in Figs. 1–3. The reactions of *n*-pentylamine and *neo*-pentylamine were predominantly to condensation products, while those of *tert*-pentylamine were to denitrogenated molecules.

The conversions to hydrocarbons (HDN) of each catalyst for each of the three amines are plotted in Fig. 4. The trend for the three pentylamine HDN reactions over MoP/SiO_2, WP/SiO_2, and MoS_2/SiO_2 catalysts is for increased reactivity in the order *neo* < *n* < *tert*. Examination of the structural properties of the amines (Table 3) shows no correlation of this order of reactivity with steric hindrance, suggesting that an S_N2 pathway is not predominant. Similarly, there is no correlation with the stability of carbocation or carbanion species, suggesting that prior scission of the amine group as in an S_N1 or E1 mechanism does not occur. However, there is a direct relationship between the order of reactivity and the number of β-hydrogens, and this suggests that C–N bond scission occurs primarily by an E2 mechanism on the catalysts (Table 4). Of course, the preferred E2 pathway is not available for *neo*-pentylamine and this molecule is likely to react by a metal-type reaction (Scheme 1). This is discussed in more depth later.

Infrared spectroscopy studies with ethylamine give insight about how the reaction proceeds. Ethylamine is the smallest member of the alkylamine family, having both α- and β-hydrogens, and is a good probe molecule for the mechanism. In this study measurements were conducted on the WP/SiO_2 catalyst because of its high activity. The catalyst was pretreated in an H_2 stream with 3000 wppm S (the same sulfur level used during reaction) to approximate the actual catalytic surface conditions. The FTIR measurements indicated that ethylamine is adsorbed on the surface of the WP/SiO_2 as an ethylammonium species. Previous studies on Mo_2C and MoS_2/SiO_2 gave similar results (28). This was deduced from the characteristic bands of this species at 2260, 2400, 2530, 2885, 2943, 2977, 3305, and 3370 cm^{-1} (29–31). The bands in the midrange region (2885–2977 cm^{-1}) are due to C–H bond symmetric and asymmetric vibrations. The weak bands at low wavenumber belong to the parent ethylamine compound (2260 cm^{-1}) and an ethylammonium species (2400–2530 cm^{-1}), while the doublet at high wavenumber (3305–3370 cm^{-1}) is also due to the ethylammonium species. The ethylamine parent is likely associated with the SiO_2 support. The IR bands on the SiO_2 are also found in the low (2260 cm^{-1}) and midrange regions (2882–2978 cm^{-1}).

TPD studies of the adsorbed ethylamine species were undertaken to understand the manner in which the reaction proceeds. Again, the studies employed the active WP/SiO_2 catalyst pretreated with 3000 ppm S. The TPD signals from the mass spectrometer are shown in Fig. 7. Ethylamine

TABLE 4

Relative Reactivities of Pentylamines According to Possible Reaction Mechanisms

Reactant	Number of β-Hydrogens	S_N1	S_N2	E1	E2
n-Pentylamine	2	Very low	High	Very low	Medium high
tert-Pentylamine	8	High	Very low	Very high	High
neo-Pentylamine	0	Very low	Very low	None	None

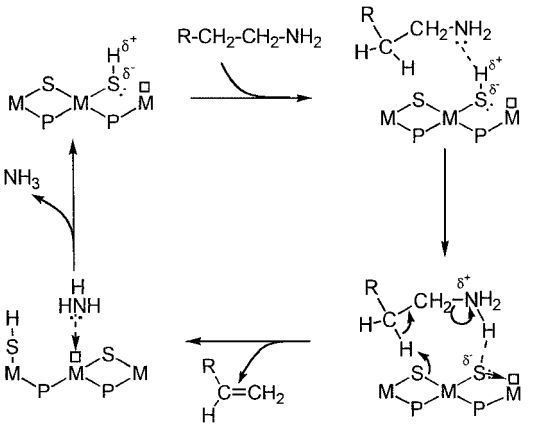

SCHEME 2. Push–pull mechanism in the HDN of an alkylamine.

desorbs molecularly in a relatively sharp peak at 380 K and a broader peak at 485 K (Fig. 7, curve a). These features probably correspond to physisorbed and chemisorbed ethylamine, respectively. The other TPD traces show that part of the adsorbed ethylamine decomposes to release ammonia and ethylene in equal proportions, but in a nonconcerted manner. Ethylene (Fig. 7, curve b) appears first at 613 K, while ammonia (Fig. 7, curve c) desorbs later at 650 K. A possible sequence of steps for the transformation is depicted in Scheme 2. In this scheme we have taken the surface of the phosphide catalyst to be populated with sulfur species which provide Brønsted acidity in the form of sulfhydril groups, as well as nucleophilic centers. The exact structure of these groups is uncertain, and the forms shown in Scheme 2 should be considered illustrative, as other possibilities exist. However, the main features of the mechanism are otherwise consistent with the observations. The amine is first protonated on a Brønsted site on the surface to adsorb as an alkylammonium species. This species then undergoes a β-hydride elimination by attack by a surface basic center. This is exactly an E2 elimination (Scheme 1) with the role of the surface now explicitly indicated, and results in the release of ethylene, as found in the TPD experiments. The eliminated ammonia interacts with the coordinatively unsaturated site on the surface and is released in a subsequent step.

Another material that has received attention as an alternate HDN catalyst is molybdenum carbide (32). Interestingly, in similar experiments using ethylamine TPD it was found that for Mo_2C (also presulfided) the adsorbed intermediate released ammonia first and then ethylene, the reverse order of the WP catalyst (28). This suggests that the nature of carbide and phosphide catalyst surfaces are quite distinct. The reactivity patterns of *n*-pentylamine and *tert*-pentylamine are consistent with the mechanism for WP/SiO_2. In particular, for *n*-pentylamine it is likely that 1-pentene was the primary reaction product as it was the major olefin product formed at low temperatures (Fig. 1, Table 2). At higher conversions the 1-pentene intermediate was hydrogenated to form *n*-pentane or isomerized by double bond migration to form *cis*- and *trans*-2-pentenes. Importantly, no *iso*pentenes were observed, indicating that carbenium ion intermediates such as those formed by S_N1 or E1 pathways were not formed. The lack of skeletal isomerization of the hydrocarbon suggests that the double bond migration step also occurred by a push–pull-type mechanism (Scheme 3). Again, in this scheme the surface structures are pictorial representations.

Thermodynamic calculations show that 2-pentene is favored over 1-pentene and *trans*-2-pentene is favored over *cis*-2-pentene. In the case of *n*-pentylamine the *cis–trans* distribution in the catalyst effluent was skewed toward 1 : 1, suggesting a kinetic control over the double bond migration step. From studies of relative stability of allylic species (33) the preference toward *cis*-2-pentene may indicate that the intermediate has partial anion character.

In the case of *tert*-pentylamine, the products of reaction were exclusively olefins and paraffins. The formation of 2-methyl-2-butene was preferred over the formation of 2-methyl-1-butene over each catalyst. This result shows preference for the thermodynamically favored triply substituted olefin product compared to the kinetically favored product having three times more available β-hydrogen atoms (6 : 2) for E2 elimination. If E1 elimination does not occur, this suggests that the methylbutenes can isomerize readily. However, it is likely in this case, because of the stability of the tertiary carbenium formed, that the S_N1 mechanism contributes to the reaction.

The reactions of *neo*-pentylamine fall into a different category from those of *n*-pentylamine and *tert*-pentylamine because the molecule does not have any β-hydrogens, making standard E1 and E2 elimination reactions impossible. Similarly, there is no γ-elimination as indicated by the absence of methylbutenes (34). As far as nucleophilic substitutions are concerned, the S_N1 route is unlikely because the intermediary primary carbenium ion is unstable, while the S_N2 pathway is blocked by steric hindrance. There is a

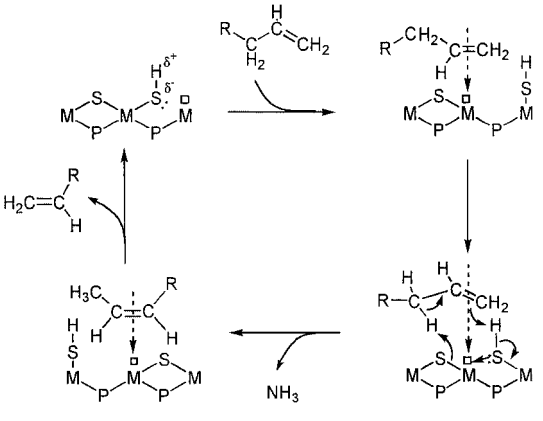

SCHEME 3. Push–pull mechanism of olefin isomerization.

possibility of hydride attack to displace the amine group, as the existence of hydride species associated with metal centers has been suggested before (35) as charged species in spillover on neutral silica supports (36) and organometallic HDN reactions involving lithium aluminum hydride (37). But again, this route appears unlikely because the hydride is likely to be held strongly. Finally, a homolytic reaction pathway can be considered involving H radicals (38, 39). This probably does not occur because of the lack of skeletal isomerization and β-scission products.

The more likely scenario in the case of *neo*-pentylamine is activation of an alpha carbon by one of the metal-centered reactions noted in Scheme 1. The aziridium-type intermediate is particularly likely. This would be followed by a series of hydrogenation and reductive elimination steps to produce the *neo*-pentane or the 2,2-dimethylpropylnitrile species. Nitriles have been reported before in the reactions of primary amines, where nitrile formation is favored by lower pressures (40) and the absence of hydrogen (41, 42). In this case, the reactive channel involving a metal-centered reaction is likely opened up at the higher temperatures of reaction needed to convert *neo*-pentylamine.

Comparison of the product distributions for the three amines shows that a significant amount of condensation products and thiols are found with *n*-pentylamine and *neo*-pentylamine. Thus, substitution is an important pathway for these molecules, especially at low temperature. In contrast, no condensation or thiol products occur for the *tert*-pentylamine HDN, indicating that elimination and hydrogenation are the only relevant reactions. In fact, the E1 mechanism is possible on *tert*-pentylamine because of the stability of the carbocation. This point is highlighted by 22% conversion of *tert*-pentylamine in a blank run at 513 K. This was the only significant background reaction noted in this investigation.

The results of this study are different from the results reported for bulk sulfides by Cattenot *et al.* (13) because ours were obtained at high pressure. Hence, we have a greater propensity for hydrogenation in this study, resulting in pentanes as well as pentenes. Interestingly, earlier results for $NiMo/Al_2O_3$ operating at 2.0 MPa yielded no condensation products (14). In particular, we operate at the same temperature (523 K), and with sulfur, but also find 2,2-dimethylpropane and condensation products in the effluent. This could be due to the presence of liquid solvent or to the nature of the catalysts.

Our results for MoS_2/SiO_2 resembled those of bulk MoS_2 used by Cattenot *et al.* (12). In particular, both had good activity for *neo*-pentylamine conversion and had similar product distributions for *n*-pentylamine conversion, including di(*n*-pentyl)amines. The presence of acid sites alone does not lead to active hydroprocessing catalysts, as demonstrated by the inactivity of alumina and silica–alumina supports, acting alone, in HDN reactions (20, 43, 44). It is relevant, though, that alumina has been reported as a catalyst for denitrogenation reactions of primary amines leading to olefins (45). The authors of the study on the alumina catalyst found that methyl substitution at the α-carbon increased the amine reaction rate, while methyl substitution at the β-carbon decreased the rate. This is in complete agreement with our findings. Thus, acid–base chemistry alone can explain results for paraffinic amines. However, good activity in hydroprocessing reactions is correlated not only with hydrogenolysis reactions but also with hydrogenation ability. The origin of the need for hydrogenation activity is related to the requirement of saturation of both the α- and β-carbon atoms in order to allow the C–N hydrogenolysis reaction to take place. It was on this basis that Nelson and Levy (11) proposed that a Hoffmann-type E2 mechanism is responsible for the C–N bond cleavage reaction. Thus the activity of catalysts toward unsaturated molecules in real feedstocks, such as quinolines, is limited by the ability of the catalyst for hydrogenation of the C6 ring. Our results confirm in a new way that C–N bond cleavage is dominated by E2 elimination. Furthermore, our interpretation of results in conjuction with acid–base chemistry is in substantial agreement with the suggestion of Topsøe *et al.* that the active centers of hydrodenitrogenation catalysts involve Brønsted acid sites (46).

In this study it was found that MoP was the least reactive in the pentylamine reactions, while WP and MoS_2 had similar activity. In contrast, in earlier work on quinoline HDN (18) it was shown that the conversions of MoP (31%) and WP (46%) were higher than that of MoS_2 (11%). It has been found in the literature that MoS_2 is active for hydrogenolysis reactions, while it is not as active for hydrogenation reactions. Our finding that MoS_2/SiO_2 was active for C–N bond hydrogenolysis reactions, but was relatively inactive for quinoline HDN, seems to support this established conclusion. The higher activity of Mo and W phosphides than the MoS_2/SiO_2 in quinoline HDN indicates that they have a distinct surface composition that gives rise to a unique reactivity. As seen in Schemes 2 and 3, our picture of the catalyst involves an amphoteric surface in which HDN elimination reactions operate by a push–pull mechanism. The amine is envisioned to adsorb from a sulfhydril Brønsted acid site by proton transfer. A nearby bridging sulfide group provides the basic site necessary for the elimination reaction. The bridging sulfide can be viewed as the conjugate base of the sulfhydril acid site. The sulfhydril site, as pictured, is intimately associated with a coordinatively unsaturated site. Thus, measurements of unsaturated sites by CO and O_2 uptake correlate indirectly to the active acid–base sites but are effective nonetheless.

Our conclusion that the HDN of alkylamines proceeds preferentially by an E2 mechanism is supported by results on heterocyclic nitrogen compounds with sulfides (47). It is found, for example, that 2-picoline is more reactive

than pyridine and 2-methylpiperidine is more reactive than piperidine, suggesting higher HDN activity for molecules with greater numbers of β-hydrogen atoms.

It has been suggested in the literature that the essential competing reaction for E2 elimination of amines involves nucleophilic substitution of sulfur upon amine groups (12–14, 48). The resulting thiol is then reported to react quickly by direct hydrogenolysis with hydrogen, forming H_2S and a *saturated* hydrocarbon. However, this does not properly explain the case of aliphatic thiol decomposition on MoS_2, in which 83% of the product of desulfurization of *n*-butylthiol was found to be olefinic and butadiene was a major product in the decomposition of tetrahydrothiophene (49). Thus, it is likely that thiols also decompose primarily by E2 elimination. It has also been reported that HDS of cyclopropylmethylthiol occurs by a free radical mechanism (50), but again, this does not explain the selectivity toward olefins noted here.

In the case of benzylamine or isoquinoline HDN reactions reported in the literature, HDN proceeds without prior hydrogenation of the C6 ring, but the process is slower (occurs at higher temperature) than in the case of aliphatic amines. This suggests that an alternate mechanism, such as one of the metal-mediated routes (metal alkyl, aziridinium ring), is available for HDN in cases where the β-carbon is not fully saturated (10, 43).

Our studies are carried out at high pressure, in the liquid phase, with a sulfur cofeed to achieve realistic conditions. The presence of sulfur likely alters the composition of the surface, possibly resulting in the formation of a surface phosphosulfide. We have indicated this in our schemes. We believe that the nature of this surface sulfide is different from that of a pure sulfide because the underlying bulk structure and morphology are different. This has been demonstrated on supported carbides and nitrides, which also form surface sulfides, but with considerably higher activities than supported sulfides (51, 52). The same thing probably happens with Mo and W phosphides, which unlike the sulfides do not have a layered structure (18) and so take on a globular morphology. This has been demonstrated recently with elegant electron microscopy work on MoP/SiO_2 (4). The spherical morphology leads to the formation of more exposed surface atoms than can be obtained with the raftlike structures in sulfides, which expose inactive basal planes. This can potentially lead to an increase in site densities for the phosphides and represents a unique opportunity for these new materials.

CONCLUSIONS

The reactivity of a series of pentylamines with different structure in HDN at high pressure confirmed the predominance of the E2 elimination mechanism in the conversion of primary amines to hydrocarbons on MoP/SiO_2, WP/SiO_2, and MoS_2/SiO_2 catalysts. Studies with ethylamine to probe the mechanism by infrared spetroscopy and TPD suggested that the reaction involved formation of adsorbed alkylammonium species and reorganization of bonds by a push–pull mechanism involving acid and base sites on the surface.

ACKNOWLEDGMENT

The authors are indebted to the Department of Energy (DOE) Office of Basic Energy Science, Grant DE-FG02-96ER14669, for financial support.

REFERENCES

1. Li, W., Dhandapani, B., and Oyama, S. T., *Chem. Lett.* 207 (1998).
2. Stinner, C., Prins, R., and Weber, Th., *J. Catal.* **191**, 438 (2000).
3. Oyama, S. T., Clark, P., Teixeira da Silva, V. L. S., Lede, E. J., and Requejo, F. G., *J. Phys. Chem.* **105**, 4961 (2001).
4. Phillips, D. C., Sawhill, S. J., Self, R., and Bussell, M. E., *J. Catal.* **207**, 266 (2002).
5. Clark, P., Li, W., and Oyama, S. T., *J. Catal.* **200**, 140 (2001).
6. Stinner, C., Prins, R., and Weber, Th., *J. Catal*. **202**, 187 (2001).
7. Robinson, W. R. A. M., van Gestel, J. N. M., Korányi, T. I., Eijsbouts, S., van der Kraan, A. M., van Veen, J. A. R., and de Beer, V. H. J., *J. Catal.* **161**, 539 (1996).
8. Wang, X., Clark, P., and Oyama, S. T., *J. Catal.*, in press.
9. Prins, R., *Adv. Catal.* **46**, 399 (2001).
10. Prins, R., Jian, M., and Flechsenhar, M., *Polyhedron* **16**(18), 3235 (1997).
11. Nelson, N., and Levy, R. B., *J. Catal.* **58**, 485 (1979).
12. Cattenot, M., Portefaix, J. L., Afonso, J., Breysse, M., Lacroix, M., and Perot, G., *J. Catal.* **173**, 366 (1998).
13. Portefaix, J. L., Cattenot, M., Guerriche, M., and Breysse, M., *Catal. Lett.* **9**, 127 (1991).
14. Portefaix, J. L., Cattenot, M., Guerriche, M., Thivolle-Cazat, J., and Breysse, M., *Catal. Today* **10**, 473 (1991).
15. Laine, R. M., *Catal. Rev.—Sci. Eng.* **25**, 459 (1983).
16. Chisholm, M. H., *Polyhedron* **16**, 3071 (1997).
17. Weller, K. J., Fox, P. A., Gray, S. D., and Wigley, D. E., *Polyhedron* **16**, 3139 (1997).
18. Clark, P., Wang, X., and Oyama, S. T., *J. Catal.* **207**, 256 (2002).
19. Hadden, S. T., and Grayson, H. G., *Hydrocarbon Process* **40**, 207 (1961).
20. Kraus, H., and Prins, R., *J. Catal.* **170**, 20 (1997).
21. Lopez Cordero, R., Esquivel, N., Lazaro, J., Fierro, J. L. G., and Lopez Agudo, A., *Appl. Catal.* **48**, 341 (1989).
22. Tauster, S. J., Pecoraro, T. A., and Chianelli, R. R., *J. Catal.* **63**, 515 (1980).
23. Tauster, S. J., and Riley, K. L., *J. Catal.* **67**, 250 (1981).
24. Bachelier, J., Duchet, J. C., and Cornet, D., *J. Phys. Chem.* **84**, 1925 (1980).
25. Bodrero, T. A., Bartholomew, C. H., and Pratt, K. C., *J. Catal.* **78**, 253 (1982).
26. Zmierczak, W., MuraliDhar, G., and Massoth, F. E., *J. Catal.* **77**, 432 (1982).
27. Katzer, J. R., and Sivasubramanian, R., *Catal. Rev.—Sci. Eng.* **20**, 155 (1979).
28. Schwartz, V., Teixeira da Silva, V., and Oyama, S. T., *J. Mol. Catal. A: Chem.* **163**, 251 (2000).
29. Parillo, D. J., Adamo, A. T., Kokotailo, G. T., and Gorte, R. J., *Appl. Catal., A* **67**, 107 (1990).
30. Zeroka, D., Jensen, J. D., and Samuels, A. C., *J. Mol. Struct.* **465**, 119 (1999).
31. Hagemann, H., and Bill, H., *J. Chem. Phys.* **80**, (1984).

32. Ramanathan, S., and Oyama, S. T., *J. Phys. Chem.* **99**, 16365 (1995).
33. Schleyer, P. V. R., Dill, J. D., Pople, J. A., and Hehre, W. J., *Tetrahedron* **33**, 2497 (1977).
34. Siddhan, S., and Narayanan, N., *J. Catal.* **59**, 405 (1979).
35. Grimblot, J., *Catal. Today* **41**, 111 (1998).
36. Stumbo, A. M., Grange, P., and Delmon, B., *Stud. Surf. Sci. Catal.* **106**, 225 (1997).
37. Weller, K. J., Fox, P. A., Gray, S. D., and Wigley, D. E., *Polyhedron* **16**(18), 3139 (1997).
38. Startsev, A. N., *J. Mol. Catal. A* **152**, 1 (2000).
39. Paul, J., Akpati, H., Nordlander, P., Oh, W. S., Goodman, D. W., and Demirel, B., *Stud. Surf. Sci. Catal.* **106**, 303 (1997).
40. Sonnemans, J., and Mars, P., *J. Catal.* **34**, 215 (1974).
41. Lee, J. H., Hamrin, C. E., Jr., and Davis, B. H., *Appl. Catal., A* **111**, 11 (1994).
42. Brey, W. S., Jr., and Cobbledick, D. S., *Ind. Eng. Chem.* **51**(9), 1031 (1959).
43. Menon, R., Joo, H. S., Guin, J. A., Reucroft, P. J., and Kim, J. Y., *Energy Fuels* **10**, 579 (1996).
44. Reinhoudt, H. R., Troost, R., van Schalkwijk, S., van Langeveld, A. D., Sie, S. T., Schulz, H., Chadwick, D., Cambra, J., de Beer, V. H. J., van Veen, J. A. R., Fierro, J. L. G., and Moulijn, J. A., *Stud. Surf. Sci. Catal.* **106**, 237 (1997).
45. Hogan, P., and Pasek, J., *Collect. Czech. Chem. Commun.* **38**, 1513 (1973).
46. Topsøe, N. Y., Topsøe, H., and Massoth, F. E., *J. Catal.* **119**, 252 (1989).
47. Cox, K. E., and Berg, L., *Chem. Eng. Prog.* **56**, 54 (1962).
48. Vivier, L., Dominguez, V., Perot, G., and Kasztelan, S., *J. Mol. Catal.* **67**, 267 (1991).
49. Kolboe, S., *Can. J. Chem.* **47**, 352 (1969).
50. Dungey, K. E., and Curtis, M. D., *J. Am. Chem. Soc.* **119**, 842 (1997).
51. Aegerter, P. A., Quigley, W. W. C., Simpson, G. J., Ziegler, D. D., Logan, J. W., McCrea, K. R., Glazier, S., and Bussell, M. E., *J. Catal.* **164**, 109 (1996).
52. McCrea, K. R., Logan, J. W., Tarbuck, T. L., Heiser, J. L., and Bussell, M. E., *J. Catal.* **171**, 255 (1997).